Heat and Technology
Vol. 32, n. 1-2, 2014

HEAT TRANSFER ANALYSIS DURING HEAT RECOVERY IN CYLINDRICAL LATENT THERMAL STORAGE UNIT

Mohamed Teggar *, El Hacene Mezaache °

*Laboratoire de Mécanique, Université Amar Telidji de Laghouat, B.P. 37G, Laghouat 03000, Algérie
°Laboratoire de Recherche sur la Physico-chimie des Surfaces et Interfaces, Université de Skikda, Algérie

ABSTRACT

In the present paper the heat transfer in a cylindrical latent heat exchanger has been analysed. Theoretical study was conducted to assess how the heat transfer is affected by the dimensionless parameters. Phase change inside the heat exchanger has been formulated by using a conduction model. An enthalpy method with finite control volume approach was used. This model has been validated by comparison with available models in literature. The influence of Biot number has been examined especially on the temperature distribution and the surface heat flux. Numerical results showed that larger Biot number leads to higher heat exchange rate, but at the beginning of the process this effect is reversed. The Biot number has no influence on the temperature distribution in the solidified PCM near the center of the cylinder. The significant influence is observed only for larger radii.

Key-words: Enthalpy method, heat storage, latent heat, PCM.

1. INTRODUCTION

The continuous increase of the level of greenhouse gas emissions and the climb of oil prices is behind the necessity of more effective utilisation of energy. Thermal energy storage is useful to correct the mismatch between the supply and demand of energy. Efficient thermal storage is a key component in thermal power systems. Among the most requirements for an efficient storage system is a good heat exchange during either heat charging and discharging. One of the most prospective techniques of thermal storage is application of Phase Change Materials (PCMs). Latent thermal storage technique is getting more attention due to high energy storage densities and smaller temperature differences as compared to sensible storage techniques. The overall concept of the storage system is the same as in solid systems, but the storing material is a material with a melting temperature within the range of the charging and discharging temperatures of the Heat Transfer Fluid (HTF). Fundamental investigations in thermal storage with PCM are aimed to give more information that can be useful for different applications such as air conditioning, solar thermal power generation [1]. A detailed review of different latent heat storage materials and systems has been carried out [2, 3 and 4].In the PCM capsule-type thermal storage systems, a HTF is used to transfer the thermal energy from the hot source to the PCM capsules (charging) and from the PCM capsules to an application system (discharging). During discharging process thermal energy is transferred from the liquid PCM as a solid layer builds up on the cold capsule wall. Stewart et al. showed that free convection can be ignored in the liquid PCM during cylindrical solidification process [5]. Saraf and Shariff [6] studied numerically the inward freezing of water in cylinders, water is initially maintained at the melting temperature and the boundary surface is maintained at a constant temperature. PCM capsules are used in waste heat recovery from chemical and metallurgical industries [7]. Esen [8] carried out a numerical study on a cylindrical latent heat storage tank. Results show that the PCM, the cylinder radius, the HTF mass flow and its inlet temperature must be chosen carefully for efficient thermal storage. Choi [9] showed that the solidification velocity is a strong function of Stefan number. Biot number had negligible effect on the phase change velocity. The problem of solidification of different PCMs (water and mixtures of water) has been investigated [10]. The materials were encapsulated in different containers (spheres and cylinders). The time necessary for total solidification has been studied. Felix [11] showed that the solid fraction and the complete thermal discharging time are strongly affected by Stefan number. Braga [12] showed that the cooling rate in cylindrical PCM solidification is a strong function of the angular position on the internal wall, the coolant temperature, the capsule material and its diameter. Kim [13] conducted a numerical study on PCM heat accumulator used in automotive field. Heat transfer characteristics during solidification of PCM were determined for circular tube systems. The effect of Biot number on the heat transfer was analysed. Heat exchange is strongly influenced by Biot number. PVC tubes filled with PCM were incorporated in a hot water tank in order to store hotness [14], by using an electrical heater during off peak hours (low cost of electrical energy). Later, the stored heat is recovered by cold water for domestic application. A parametric study was carried out to optimise the PCM distribution inside the hot water tank. Good knowledge on characteristics and energy performance of PCM is essential for researchers and practitioners. The present analysis can be useful for the design and optimisation of the thermal storage system. The

latent thermal storage consists of a set of cylindrical tubes distributed equally in the storage volume (fig. 1). PCM is tanked in cylinders and HTF flows parallel to them. Heat is transferred from the storage to the sink to cope with a demand.

2. PHYSICAL SITUATION

Consider one cell of the heat accumulator (fig. 1), a cylinder of diameter D filled with a liquid pure PCM at an arbitrary initial uniform temperature $T_i > T_f$. The container wall is so thin and of a so conductive material that the thermal resistance through the wall is negligible. The HTF is considered to be flowing with a constant temperature T_∞, which is lower than the PCM melting temperature. The HTF does not change its temperature when looking at a small portion of the cylinder. The heat transfer coefficient h is supposed constant. Gravitational effects are not considered during solidification of PCM. Therefore, liquid and solid densities are supposed constant and equal. The solidification problem is controlled by pure conduction since natural convection has a negligible effect unlike the melting probleme. Thus, during the heat discharging process, the main heat transfer mode in the storage medium is conduction. The same boundary condition around the cylinder results in independency of dependant variables in respect to the angle, thus the problem may be studied in one dimension i.e. r-direction. Considering the symmetry of the configuration, the computational domain of the problem can be reduced to $0 \le r \le D/2$.

Therefore, inward solidification process of the PCM is described, using the enthalpy formulation, by:

$$\frac{\partial H}{\partial t} = \left[\frac{1}{r}\frac{\partial}{\partial r}\left(rk\frac{\partial T}{\partial r}\right)\right] \tag{1}$$

With the initial and boundary conditions:

$$T(r, t=0) = T_{in} \tag{2}$$

For t>0:

$$\left.\frac{\partial T}{\partial r}\right|_{r=0} = 0 \tag{3}$$

$$-k\left.\frac{\partial T}{\partial r}\right|_{r=D/2} = h(T_w - T_\infty) \tag{4}$$

With:

$$T_w = T(r = D/2, t) \tag{5}$$

If the enthalpy is the sensible heat in the solid, in the liquid phase it is the sum of the sensible and latent heat:

$$H = \begin{cases} \rho c_s (T - T_f) & \text{(solid)} \\ \rho c_l (T - T_f) + \rho L_f & \text{(liquid)} \end{cases} \tag{6}$$

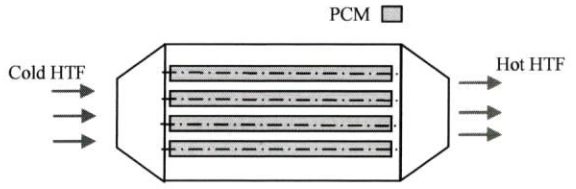

Figure 1. Schematic of the latent heat accumulator

Solving for T:

$$T = \begin{cases} T_f + \dfrac{H}{\rho c_s} & H \le 0 \quad \text{(solid)} \\ T_f & 0 < H < \rho L_f \quad \text{(interace)} \\ T_f + \dfrac{H - \rho L_f}{\rho c_l} & H \ge \rho L_f \quad \text{(liquid)} \end{cases} \tag{7}$$

This model is appropriate for pure materials or eutectics in which phase change occurs at a constant temperature.

Dimensionless coordinate, time and physical properties are chosen:

$$R = \frac{r}{(D/2)}, \quad \tau = \frac{\alpha_s t}{(D/2)^2}, \quad k^* = \frac{k}{k_s}, \quad c^* = \frac{c}{c_s}$$

Dimensionless temperature and enthalpy are defined as follows:

$$\theta = \frac{T - T_\infty}{T_{in} - T_\infty}, \quad H^* = \frac{H}{\rho_s c_s (T_{in} - T_\infty)}$$

The dimensionless parameters are then:

$$Bi = \frac{h\,(D/2)}{k_s}, \quad Ste = \frac{c_s (T_{in} - T_\infty)}{L_f}$$

Thus, the model can be written:

$$\frac{\partial H^*}{\partial \tau} = \left[\frac{1}{R}\frac{\partial}{\partial R}\left(Rk^*\frac{\partial \theta}{\partial R}\right)\right] \tag{8}$$

$$\theta(R, \tau = 0) = 1 \tag{9}$$

For τ>0 :

$$\left.\frac{\partial \theta}{\partial R}\right|_{R=0} = 0 \tag{10}$$

$$\left.\frac{\partial \theta}{\partial R}\right|_{R=1} = -Bi\,\theta_w \tag{11}$$

Where $\theta_w = \theta(R = 1, \tau)$

$$H^*(\theta)=\begin{cases}\theta-\theta_f \\ c^*(\theta-\theta_f)+\dfrac{1}{Ste}\end{cases}\quad\text{for}\quad\begin{cases}\theta<\theta_f \\ \theta>\theta_f\end{cases} \tag{12}$$

$$\theta=\begin{cases}H^*+\theta_f \\ \theta_f \\ \left(H^*-1/Ste\right)/c^*+\theta_f\end{cases}\quad\text{for}\quad\begin{cases}H^*<0 \\ 0\le H^*\le 1/Ste \\ H^*>1/Ste\end{cases} \tag{13}$$

3. NUMERICAL PROCEDURE

The numerical solution was realised using the finite control volume approach. The computational domain ($0\le R\le 1$) was partitioned into 41 of control volumes, with each control volume V_i (i=1, 2,..n), we associate a node (P) a point in the center of V_i. Except the first control volume at R=0 which is $\Delta R/2$ width, the partition is uniform with $\Delta R=R/(n\text{-}0.5)$. The time increment is optimised and chosen $\Delta\tau$ =0.000 1.

We applied the energy conservation equation to each control volume to obtain a discrete heat balance, and we used it to update the enthalpy H^*_i of each control volume [15].

We multiply eq. (8) by R.

$$\frac{\partial H^*}{\partial\tau}R=\left[\frac{\partial}{\partial R}\left(Rk^*\frac{\partial\theta}{\partial R}\right)\right] \tag{14}$$

And integrating over V_i between τk and τ_{k+1}:

$$\int_k^{k+1}\int_{R_e}^{R_w}\frac{\partial H^*}{\partial\tau}RdRd\tau=\int_k^{k+1}\int_{R_e}^{R_w}\left[\frac{\partial}{\partial R}\left(Rk^*\frac{\partial\theta}{\partial R}\right)\right]dRd\tau \tag{15}$$

Assuming that V_i is small enough for H^*_i to be approximated by the mean enthalpy inside the control volume at a given time level. We suppose the peace-wise linear variation of the temperature between two adjacent control volumes.

$$\int_k^{k+1}\frac{\partial H^*}{\partial\tau}\frac{R_w^2-R_e^2}{2}d\tau=\left(H_p^{*k+1}-H_p^{*k}\right)\frac{R_w^2-R_e^2}{2} \tag{16}$$

$$\int_k^{k+1}\int_{R_e}^{R_w}\left[\frac{\partial}{\partial R}\left(Rk^*\frac{\partial\theta}{\partial R}\right)\right]dRd\tau=\int_{R_e}^{R_w}\left[\frac{\partial}{\partial R}\left(Rk^*\frac{\partial\theta}{\partial R}\right)\right]\Delta\tau dR$$

$$=\left(R_wk^*\left.\frac{\partial\theta}{\partial R}\right|_w-R_ek^*\left.\frac{\partial\theta}{\partial R}\right|_e\right)\Delta\tau$$

$$=\left(R_wk^*\frac{\theta_W-\theta_P}{\Delta R}-R_ek^*\frac{\theta_P-\theta_E}{\Delta R}\right)\Delta\tau \tag{17}$$

It follows:

$$\left(H_p^{*k+1}-H_p^{*k}\right)\frac{R_w^2-R_e^2}{2}=\left[\left(R_wk^*\frac{\theta_W-\theta_P}{\Delta R}-R_ek^*\frac{\theta_P-\theta_E}{\Delta R}\right)\right]\Delta\tau \tag{18}$$

Where R_w and R_e are functions of i :

$R_w=(i-0.5)\Delta R$ for i = 1,...,41

$R_e=(i-1.5)\Delta R$ for i = 2,...,41

$R_e=0$ for i = 1

$$H_p^{*k+1}=H_p^{*k}+\frac{2\Delta\tau}{\left(R_w^2-R_e^2\right)}\left[\left(R_wk^*\frac{\theta_W-\theta_P}{\Delta R}-R_ek^*\frac{\theta_P-\theta_E}{\Delta R}\right)\right] \tag{19}$$

Replacing P by i and using time explicit scheme, we obtain:

$$H_i^{*k+1}=H_i^{*k}+\frac{2\Delta\tau}{\left(R_w^2-R_e^2\right)}\left[\left(R_wk^*\frac{\theta_{i+1}^k-\theta_i^k}{\Delta R}-R_ek^*\frac{\theta_i^k-\theta_{i-1}^k}{\Delta R}\right)\right] \tag{20}$$

All grid points obey this algorithm except for the first and the last nodes where boundary conditions should be taken into account, so for the first and the last nodes respectively:

$$H_1^{*k+1}=H_1^{*k}+\frac{\Delta\tau}{(\Delta R/2)^2}K^*\left(\theta_2^k-\theta_1^k\right) \tag{21}$$

$$H_n^{*k+1}=H_n^{*k}+\frac{2\Delta\tau}{\mathrm{R}_w^2-R_e^2}\left[-\mathrm{R}_wBi\theta_s^k-\mathrm{R}_ek^*\frac{\left(\theta_n^k-\theta_{n-1}^k\right)}{\Delta R}\right] \tag{22}$$

With θ_s the dimensionless temperature at the surface of the cylinder.

$$H_n^{*k+1}=H_n^{*k}+\frac{2\Delta\tau}{\mathrm{R}_w^2-R_e^2}\left[-\frac{2Bik^*}{2k^*+Bi\Delta R}\mathrm{R}_w\theta_n^k-\mathrm{R}_ek^*\frac{\left(\theta_n^k-\theta_{n-1}^k\right)}{\Delta R}\right] \tag{23}$$

Explicit scheme was used in numerical calculations. In the enthalpy method, this technique generates some oscillations in nodal temperature values during the solidification process. However, when the total grid number inside the PCM is increased, there was a reduction in numerical fluctuations in temperature values. Bilir and Ilken [16] obtained stable results with 41 control volumes ($0\le R\le 1$). In addition, numerical oscillations were affected by Stefan number. For smaller values, the time step must be smaller which resulted in increasing number of control volumes. Figure 2 shows this effect on the heat transfer rate.

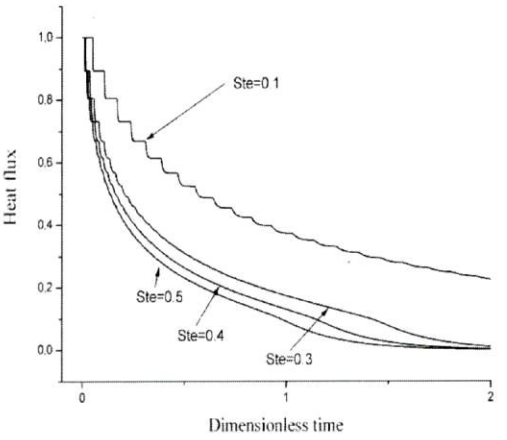

Figure 2. Effect of Stefan number on the numerical results

4. RESULTS

Validation of the numerical predictions has been done by comparison to numerical results available in literature. The first comparison was made with the numerical model of Bilir and Ilken [16] for the solidification of PCM in a cylinder capsule. The results were obtained for a cylinder with constant temperature boundary condition at the surface. Therefore, a very big Biot number is chosen (Bi=100) to made the comparison possible. Figure 3 shows a very good agreement between the two models, the method used in both studies is the same (enthalpy method and control volume approach). Figure 4 shows another comparison between the present model and the results due to Tao [17].The author studied inward cylindrical solidification in which the liquid PCM is initially at the melting temperature. As can be seen (fig.4), the agreement between the two results was very good. The parameters controlling transient conduction associated with phase change and convective boundary are Stefan and Biot numbers. The temperature history at the center and the surface of the PCM is presented in figure 5. Solid PCM builds up as the latent heat is released isothermally at the solid-liquid interface.

A jump in the enthalpy function could be observed during phase change (fig. 6). The released heat is removed by conduction in the solidified mass to the colder surface of the cylinder. Then heat is transferred from the outer surface of the cylinder to the HTF. When liquid becomes fully solid, temperature begins to decrease more rapidly with sensible heat exchange until it reaches thermal equilibrium with the liquid HTF.

The heat flux through solid PCM region was analysed. The heat flux at the surface of the cylinder is presented in figure 7. The model ignored the sensible heat contributions at the beginning of solidification, in other words the initial temperature of PCM was set equal to the melting temperature. The inclusion of the sensible heat is sometimes useful since various PCMs have significant sensible heat capacities which enhance the overall thermal storage capacity. The heat flux (fig. 7) decreases with increasing time.

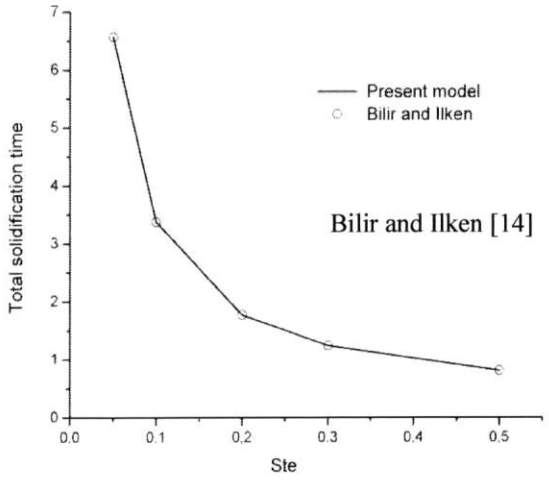

Figure 3. Comparison of the present model with results of Bilir and Ilken [14]

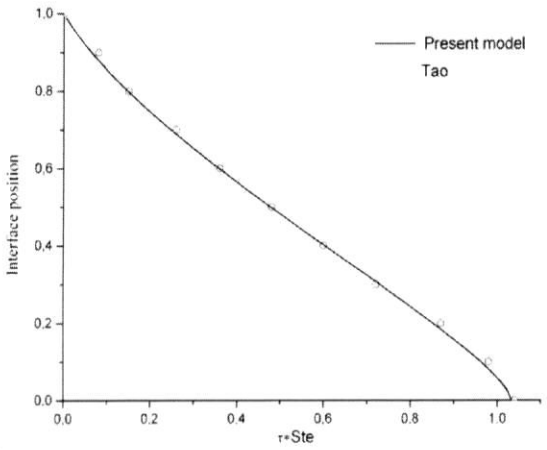

Figure 4. Comparison of the present model with the results due to Tao [15]

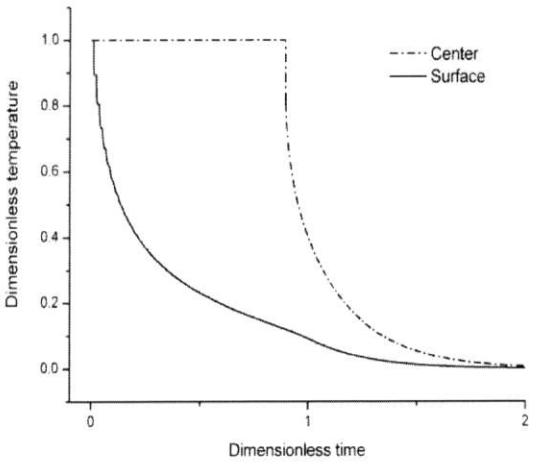

Figure 5. Temperature history at the center and the surface of the cylinder

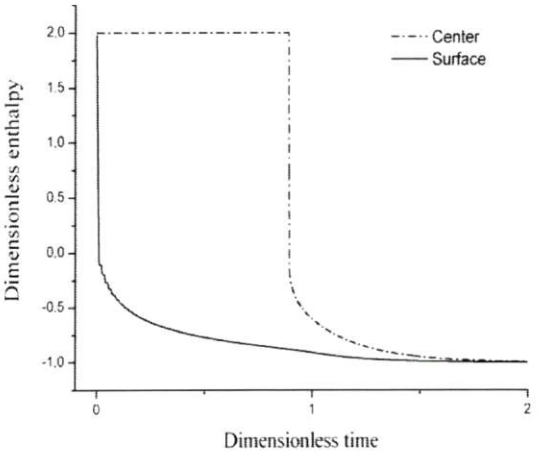

Figure 6. Enthalpy history at the center and the surface of the cylinder

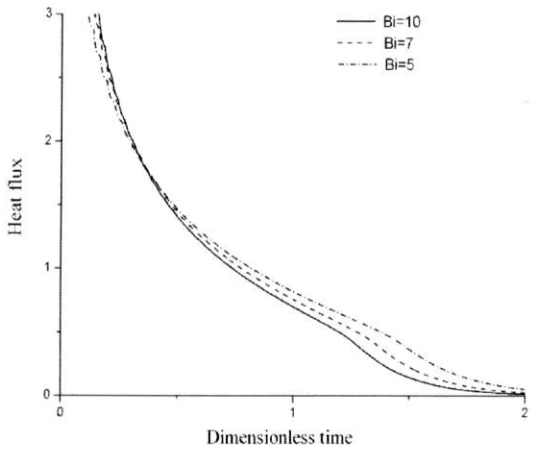

Figure 7. Heat flux at the surface of the cylinder

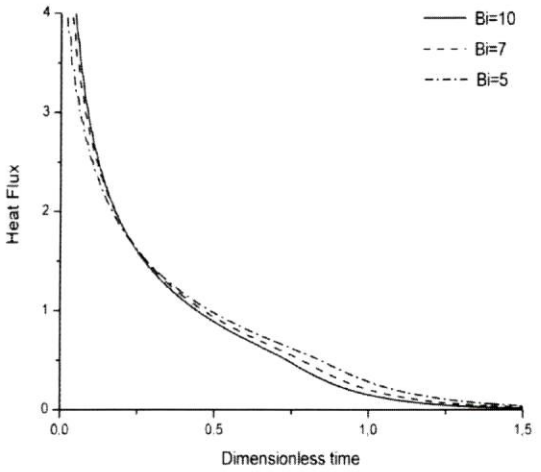

Figure 8. Heat flux at the surface of the cylinder (Ste=0.6)

The heat flux rate changed rapidly at the beginning, but rather slowly later on. Thermal resistance increased with increasing the thickness of the solidified layer, thus diminishing heat transfer rate. The rate of heat transfer changed slightly after complete solidification of the cell. One could state the influence of the liquid fraction on the heat transfer. We could also observe that the larger the Biot number the higher the heat transfer rate. A large value of Bi indicates that the phase change would be done in a short time. But at the beginning of the process, this influence was reversed. The same observation was found with a bigger value of Stefan number *Ste*=0.6 (fig. 8). The maximum energy exchanged would be reached when the system reaches thermal equilibrium with the temperature of the HTF.

In figure 9 dimensionless temperature is plotted against *R* with Bi as parameter for the values (5, 7 and 10), and this at the moment when phase change is completely done. Results showed that the temperatures in solid region decreased with *R*. The Biot number had no influence on the temperature distribution in the solid region near the center of the cylinder. The significant influence of Biot number was observed only for larger values of *R*. Larger Biot number resulted in larger temperature difference in the solidified region. Hence, the gradients would be important. Small Biot number represents small resistance to heat conduction, as a result small temperature gradients within the solidified mass. Common PCMs are known for their low thermal conductivity (i. e. large *Bi*). Therefore, large temperature differences occur between the inner and outer regions of large cylinders.

Figure 10 shows the variation of the solidified mass fraction in terms of time. The solidified mass fraction was calculated based upon the interface position. Tracking the phase change front by the enthalpy method is based on values taken by the enthalpy function. Where a controlling value corresponding to phase change is used to decide whether a point is in liquid, mushy or solid state. It was observed that near the center of the cylinder the slope was very becomes large. That was due to the reduced heat exchange area as the liquid-solid interface position moved inwards.

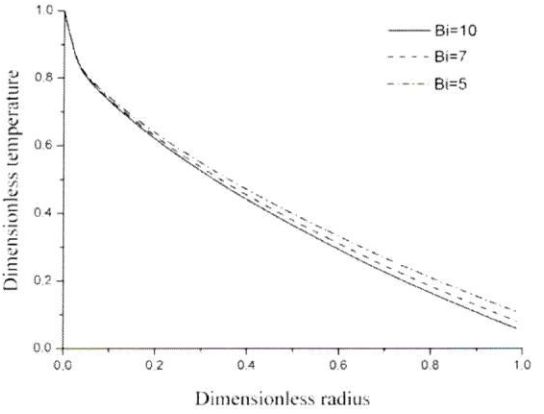

Figure 9. Temperature profile in the solidified PCM

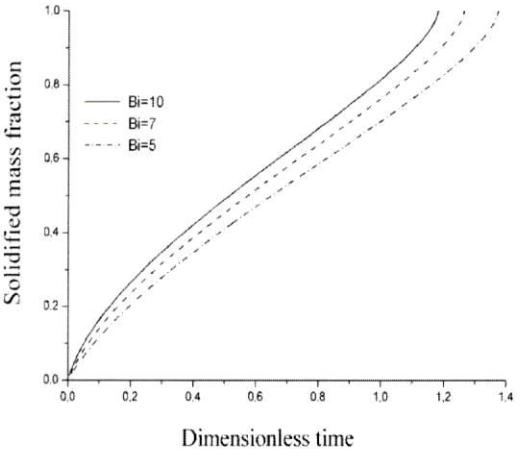

Figure 10. Solidified mass fraction versus dimensionless time

5. CONCLUSION

A conduction model describing inward solidification of a phase change material in a latent heat storage unit is presented. The numerical predictions were consistent and compare well with available results reported in literature. Larger Biot number resulted in larger heat exchange rate but at the beginning of the processes the typical effect was reversed. Near to the center of the cylinder in the solidified PCM, the Biot number had no influence on the temperature distribution. The significant influence was observed only for larger radii.

6. NOMENCLATURE

Bi	Biot number	
c	Specific heat	(J/kg °C)
D	Diameter of the cylinder	m
h	Heat convection coefficient	(W/m^2 °C)
H	Specific enthalpy	(J/kg)
k	Thermal conductivity	(W/m °C)
L_f	Latent heat of melting	(J/kg)
Ste	Stefan number	
T	Temperature	°C
t	Time	s
r	Cylinder radius	m
R	Dimensionless radius	
α	Thermal diffusivity	(m^2/s)
θ	Dimensionless temperature	
ρ	Density	(kg/m^3)
τ	Dimensionless time	

Subscripts

∞	coolant HTF
c	complete solidification
f	melting
in	initial
l	liquid
s	solid
w	wall

7. REFERENCES

1. G. Cammarata, L. Monaco, l. Cammarata and G. Petrone, A Numerical Procedure for PCM Thermal Storage Design in Solar Plants, *Int. J. Heat and Technology*, vol. 31 (2), pp. 105-110, 2013.
2. L.F. Cabeza et al., Materials Used as PCM in Thermal Energy Storage in Buildings: A review, *Renewable and Sustainable Energy Reviews*, vol. 15, pp. 1675-1695, 2011.
3. M. Pomianowski, P. Heiselberg and Y. Zhang, Review of Thermal Energy Storage Technologies Based on PCM Application in Buildings, *Energy and Buildings*, vol. 67, pp. 56-69, 2013.
4. N. Soares, J. J. Costa, A.R. Gaspar and P. Santos, Review of Passive PCM Latent Heat Thermal Energy Storage Systems Towards Buildings Energy Efficiency, *Energy and Buildings*, vol. 59, pp. 82-103, 2013.
5. W.E. Stewart and K.L. Smith, Experimental Inward Solidification of Initially Superheated Water in a Cylinder, *Int. Comm. Heat Mass Transfer*, vol. 14, pp. 21-31, 1987.
6. G. R. Saraf and L. K. A. Sharif, Inward Freezing of Water in Cylinders, *Int.J. Refrig*, vol. 10, pp. 342-348, 1987.
7. J. Yagi and T. Akiyama, Storage of Thermal Energy for Effective use of Waste Heat from Industries, *Journal of Materials Processing Technology*, vol. pp. 793-804, 1995.
8. M. Esen and T. Ayhan, Development of a Model Compatible with Solar Assisted Cylindrical Energy Storage Tank and Variation of Stored Energy with Time for Different Phase Change Materials, *Energy Convers. Mgmt*, vol. 37 (12), pp. 1775-1785, 1996.
9. J. C. Choi, S. D. Kim and G. Y. Han, Heat Transfer Characteristics in Low-Temperature Latent Heat Storage Systems Using Salt-hydrates at Heat Recovery Stage, *Solar Energy Materials and Solar Cells*, vol. 40, pp. 71-87, 1996.
10. K.A.R. Ismail and R.I.R. Moraes, A Numerical and Experimental Investigation of Different Containers and PCM Options for Cold Storage Modular Units for Domestic Applications, *International Journal of Heat and Mass Transfer*, vol. 52, 4195-4202, 2009.
11. A. F. Regin, S.C. Solanki and J.S. Saini, An Analysis of a Packed Bed Latent Heat Thermal Energy Storage System Using PCM capsules: Numerical Investigation, *Renewable Energy*, vol. 34, pp. 1765-1773, 2009.
12. S. L. Braga et al., A Study of Cooling Rate of the Supercooled Water Inside of Cylindrical Capsules, *International Journal of Refrigeration*, vol. 32, pp. 953-959, 2009.
13. K. Kim et al., Feasibility Study on a Novel Cooling Technique Using a Phase Change Material in an *Automotive Engine*, Energy, vol. 35, pp. 478-484, 2010.
14. A. de Gracia et al., Thermal analysis of including phase change material in a domestic hot water cylinder, *Applied Thermal Engineering*, vol. 31, pp. 3938-3945, 2011.
15. M. Teggar, E. Mezaache, A. Benchatti and B. Zeghmati, Comparative Study of Heat Transfer during Solidification of Phase Change Materials inside Three Different Capsules, *Int. J. Heat and Technology*, vol. 28 (2), pp. 17-22, 2010.
16. B. Levent and Z. Ilken, Total Solidification Time of a Liquid Phase Change Material Enclosed in Cylindrical/Spherical Containers, *Applied Thermal Engineering*, vol. 25, pp. 1488-1502, 2005.
17. L. C. Tao, Generalized Numerical Solutions of Freezing a Saturated Liquid in Cylinders and Spheres, *A. I. CH. Journal*, vol. 13 (1), pp. 165-169, 1967.